NUWC-NPT Technical Report 10,400
1 September 1994

A Low-Dimensional Structural Model of a Turbulent Boundary Layer Separating Intermittently in Space

P. R. Bandyopadhyay
Weapons Technology and Undersea Systems Department

Naval Undersea Warfare Center Division
Newport, Rhode Island

PREFACE

Publication of this report was supported by the Naval Undersea Warfare Center Division, Newport, Rhode Island, Code 10.

The technical reviewer for this report was J. R. Grant (Code 8233). The author thanks him for the many suggestions he offered.

The author also acknowledges the helpful comments of S. A. Huyer (Code 8233).

Reviewed and Approved: 1 September 1994

F. L. White
Head, Weapons Technology and
Undersea Systems Department

REPORT DOCUMENTATION PAGE

Form Approved
OMB No. 0704-0188

1. AGENCY USE ONLY *(Leave blank)*	2. REPORT DATE	3. REPORT TYPE AND DATES COVERED
	1 September 1994	

4. TITLE AND SUBTITLE

A Low-Dimensional Structural Model of a Turbulent Boundary Layer Separating Intermittently in Space

5. FUNDING NUMBERS

6. AUTHOR(S)

P. R. Bandyopadhyay

7. PERFORMING ORGANIZATION NAME(S) AND ADDRESS(ES)

Naval Undersea Warfare Center Division
1176 Howell Street
Newport, Rhode Island 02841-1708

8. PERFORMING ORGANIZATION REPORT NUMBER

TR 10,400

9. SPONSORING/MONITORING AGENCY NAME(S) AND ADDRESS(ES)

10. SPONSORING/MONITORING AGENCY REPORT NUMBER

11. SUPPLEMENTARY NOTES

12a. DISTRIBUTION/AVAILABILITY STATEMENT

Approved for public release; distribution is unlimited.

12b. DISTRIBUTION CODE

13. ABSTRACT (Maximum 200 words)

The phenomenon of intermittent separation occurring in space on a smooth, flat plate in an incompressible turbulent boundary layer, subjected to an adverse pressure gradient barely strong enough to cause separation, is described. The effect of adverse pressure gradient on a hairpin vortex is analyzed, and the process of liftup of the near-wall vorticity to be expected during separation is discussed. These effects are then compared with the results of an experiment that explores the organized nature of the process of intermittency occurring in incipient separation. Subsequently, a low-dimensional structural model of the phenomenon of intermittency occurring in incipient separation, based on a limited number of large structures, is developed, and a comparison with the measurements of separation intermittency is made. The potential usefulness of the model to an artificial neural network for predicting the time-dependent separation process is discussed. The most important result of the proposed structural model is that there is a sequence of large structures involved in the separation process and that this sequence has a regular attractor. It is proposed that the features of the separation process are related to chaos theory.

14. SUBJECT TERMS

Active Turbulence Control
Adverse Pressure Gradients
Artificial Neural Networks
Chaos Theory
Turbulent Boundary Layers
Fluid Mechanics

15. NUMBER OF PAGES
42

16. PRICE CODE

17. SECURITY CLASSIFICATION OF REPORT	18. SECURITY CLASSIFICATION OF THIS PAGE	19. SECURITY CLASSIFICATION OF ABSTRACT	20. LIMITATION OF ABSTRACT
Unclassified	Unclassified	Unclassified	SAR

TABLE OF CONTENTS

LIST OF ILLUSTRATIONS

LIST OF ILLUSTRATIONS (Cont'd)

A LOW-DIMENSIONAL STRUCTURAL MODEL OF A TURBULENT BOUNDARY LAYER SEPARATING INTERMITTENTLY IN SPACE

1. INTRODUCTION

During the last four decades, much effort has been devoted to the investigation of the quasi-organized nature of turbulent shear flows. It is hoped that the knowledge gained from these efforts will be useful in controlling turbulence and in developing structural models of turbulence. In turbulent boundary layers, some progress has been made only in the development of structural models (Bandyopadhyay and Balasubramanian, 1993 and 1994a, and Perry et al., 1991). However, because both structural models and active turbulence control strategies use the distilled knowledge of the organized structures, any progress in structural modeling should significantly facilitate the development of active turbulence control schemes.

Active control schemes are potentially more beneficial than passive schemes. However, a number of problems are thwarting the practical development of active schemes of controlling turbulence in a turbulent boundary layer. One of these problems relates to the dimension of the flow's unsteadiness. Dimension is the number of structures required to model a turbulence phenomenon. In the work by Bandyopadhyay and Balasubramanian (1993 and 1994a), the dimension is 1 because only one three-dimensional elliptic vortex in a unit-flow domain is used to model the second and third moments of turbulence in the outer layer. In the present work, the dimension is 6 or 7 (<10) because that many large structures are required to describe the phenomenon of intermittent separation. Obviously, the turbulence control task would be much more tractable if the dimension of the system is small. The success of the structural models basically demonstrates the low dimension of the system and, therefore, these models have an appeal to active turbulence control. This report presents a structural model of a turbulent boundary layer over a smooth, flat plate that separates intermittently in space because of an imposed weak, adverse pressure gradient. The utility of the model lies in its low-dimensional nature and the consequent implication to active turbulence control and chaos theory.

Because of its adverse effects on drag, the phenomenon of boundary-layer separation continues to be of practical interest. The separation control techniques and the detailed turbulence structure in separating turbulent boundary layers have been reviewed, respectively, by Gad-el-Hak and Bushnell (1991) and Simpson (1985). In the control techniques, the focus has been on the entire shear flow, rather than on the constituent turbulence structures. While Simpson (1985) has collected a notable amount of experimental information on the structure, any analysis of the separation process based on the turbulence structure is lacking.

In a turbulent boundary layer subjected to an adverse pressure gradient at a given ratio of the displacement thickness δ^* to the local boundary-layer thickness δ, the separation characteristic depends on the value of the shape factor H, which is the ratio of δ^* to the momentum thickness θ. At values of H that are barely large enough to cause separation, the point of separation intermittently moves back and forth over the surface. However, as H is increased, the boundary-layer separation becomes full (Simpson et al. (1977), Perry and Schofield (1973), and Sandborn and Kline (1961)).

The phenomenon of intermittent separation occurring in space on a smooth, flat plate in an incompressible turbulent boundary layer is the subject of this paper. Studies on turbulent boundary layers negotiating a backward facing step have shown that the point of reattachment also fluctuates back and forth over the surface, an occurrence that is attributable to the quasi-periodic passage of large structures in the mixing layer that develops in the detached layer (Eaton and Johnston (1981), Driver et al. (1987), and Bandyopadhyay (1991)). Thus, there are some hints that the process of intermittency occurring in incipient separation, which is also presumably of low-frequency in nature, could likewise be governed by the passage of large-scale structures. This line of query has been pursued in this work.

This report first analyzes the effects of adverse pressure gradient on a hairpin vortex and discusses the process of the near-wall vorticity liftup to be expected during separation. These effects are then compared with the results of an experiment that explores the organized nature of the process of intermittency occurring in incipient separation. Subsequently, a low-dimensional structural model of the phenomenon of intermittency occurring in incipient separation, based on a limited number of large structures, is developed, and a comparison with the measurements of separation intermittency is made. The potential usefulness of the model to an artificial neural network for predicting the time-dependent separation process is also briefly discussed. Most importantly, this report shows that this separation process relates to the concepts of nonlinear dynamics/chaos theory.

2. STRUCTURE OF TURBULENCE DURING INCIPIENT SEPARATION

2.1 ROTATION AND STRETCHING OF HAIRPIN VORTICES CAUSED BY ADVERSE PRESSURE GRADIENT

The outer-layer effects of the pressure gradient can be predicted by subjecting the constituent hairpin vortices of a zero pressure gradient boundary layer to adverse pressure gradients based on kinematics alone (Bandyopadhyay, 1980). Such an approach accurately shows how the 20° upstream interface of certain large structures is formed in a zero pressure gradient flow when the hairpin vortices are produced at the wall at regular intervals because of a passing sublayer instability wave.

Near the region of separation, within an eddy length of $L = \delta = 24$ cm, for example, the typical time of flight in the adverse region of pressure gradient is $0.24/1.2 = 0.2$ s because the freestream velocity near separation is 1.2 m/s. From Simpson et al. (1977), the u-turbulence intensity is approximately 14 percent in the outer layer close to the region of separation. The turbulence distortion time within L is thus 1.4 s (= 24 cm /(120 cm/s x 0.14)). Because this turbulence distortion time is larger than the mean flow distortion time by a factor of 7, the distortion is deemed rapid, and the dynamics of a characteristic eddy is then treated accordingly.

Now, consider the line of vorticity ω where P and Q are two neighboring points as shown in figure 1(a) (Batchelor, 1967, p. 268). Assume that Q is subjected to a relative velocity of δU with respect to P. The component of δU along PQ is responsible for the extension or contraction of the vortex line, whereas the normal component causes the vortex to rotate like a rigid body. (Here, only one vortex line is being considered.) On the other hand, as shown in figure 1(b), a hairpin vortex has a pair of vortex lines, and the rotation induced by the boundary-layer mean shear is countered by the induced velocity between the two legs acting normal to the plane on which the legs lie (Bandyopadhyay, 1980). Because the pressure gradient is being applied abruptly, the viscous effects can be ignored (Batchelor and Proudman, 1954). Just before such a pressure gradient is applied, consider an ideal hairpin vortex at $\alpha = 45°$ to the flow direction as shown in figure 1(b), which is the mean preferred orientation in a zero pressure gradient turbulent boundary layer. Let U be its convection velocity, and U_{rl} and U_{sl} be the respective rotational and stretching components. It is assumed that the convection velocity acts in the outer layer, and the hairpin vortex is anchored near the wall. The velocities are related as

$$U_{rl} = U \sin \alpha,$$
$$U_{sl} = U \cos \alpha, \qquad (1)$$

where for $\alpha = 45°$, $U_{rl} = 0.7U$, and $U_{sl} = 0.7U$.

Consider an adverse pressure gradient that is suddenly applied in such a way that the convection, rotational, and stretching velocities are reduced by a factor η while α is still 45°. Then the immediate effect of the adverse pressure gradient is a uniform reduction of the two components, namely, reduced rotation and stretching by a factor of η. The reduced rotational

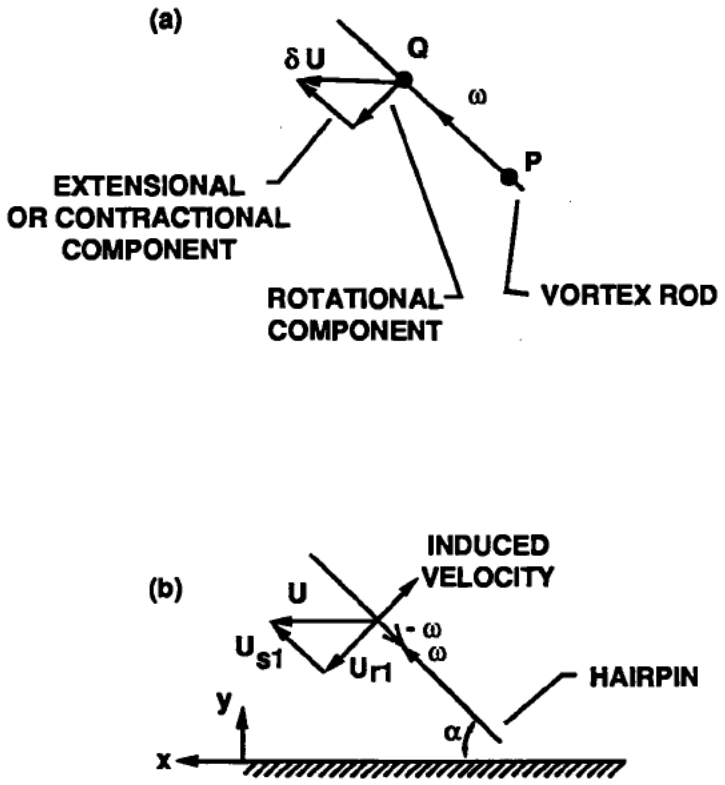

Figure 1. (a) Two-Dimensional Vortex Line and (b) Inclined Hairpin Vortex

component will upset the equilibrium and allow α to increase above 45° because of the pre-existing induced velocity of the hairpin vortex. Therefore, in adverse pressure gradients, $\alpha > 45°$ is of greater interest, and as the point of separation is approached, the net rotational part remains as the stretching part (compression) reduces. (A favorable pressure gradient has an opposite effect (Bandyopadhyay, 1989a).)

2.2 STRUCTURE IN THE OUTER REGION

Because the convection velocity in the outer layer is a constant fraction of the local freestream velocity, the successive large structures in an adverse gradient flow (shown schematically in figure. 2) will have decreasing convection velocities: $U_{c1} > U_{c2} > U_{c3}$, and so on. This reduces the intervening extents of the irrotational flow with x, that is, $\Delta x_1 > \Delta x_2$, and so on. With $\alpha \rightarrow 90°$ simultaneously as separation is approached, the result is a rapid increase in δ attributable not entirely to entrainment as is commonly the case, but to a ***reorientation*** of the hairpin vortices. This seems to partly explain why the thicknesses δ^*, θ, and δ are under-computed near separation (Bandyopadhyay, 1989a) (see figure 12). The net effect is an outward shift in the mean location of the intermittent layer, whose width also decreases. This result is what Fiedler and Head (1966) have measured and also agrees with Simpson et al. (1977), who measured that the frequency of the turbulent bulges decreases as separation is approached.

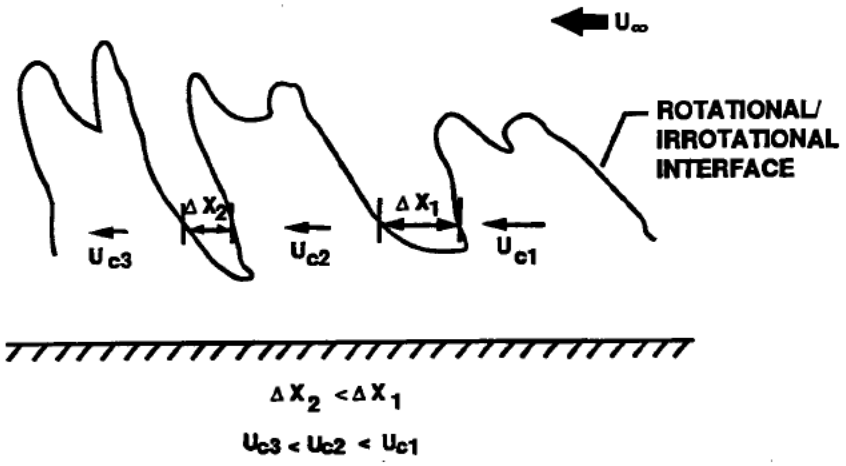

Figure 2. Schematic of the Compression of the Outer-Layer Irrotational Patches in Adverse Pressure Gradient Flows

2.3 STRUCTURE IN THE NEAR-WALL REGION

The structure of the wall region of the separating boundary layer can be better understood by considering the region of adverse pressure gradient as a region of vorticity sink (Lighthill, 1963, p. 69). In a two-dimensional flow (0, 0, ω_z), at $y = 0$, the vorticity equation reduces to

$$\frac{1}{\rho}\frac{\partial p}{\partial x} + \nu\frac{\partial \omega_z}{\partial y} = 0 \quad , \tag{2}$$

where $\omega_z = -\partial U / \partial y$, ρ is density, p is pressure, and x, y, z are the longitudinal, surface-normal and spanwise distances, respectively. The pressure gradient along the wall and the vorticity gradient normal to the wall are thus related, and the relationship might apply very close to the wall also (Tritton, 1988, p. 142). (The streamwise distribution of ω_z at the wall in separating flows is schematically shown in figure 4c. The mean point of separation is shown by the symbol S and beyond that, there is a region of reversed vorticity.) Recently, Andreopoulos and Agui (1994) have made use of equation (2) to draw inferences about vorticity flux at the wall from very closely spaced wall pressure sensors of five wall units in diameter. They have shown that the vorticity flux away from the wall remains inclined to the wall at 45° ± 5° to the flow direction, which is the preferred orientation of the hairpin vortices in a zero pressure gradient turbulent boundary layer (Head and Bandyopadhyay, 1981).

The existence of vorticity in discrete regions in a turbulent boundary layer implies that they are formed from a vorticity layer that is also nonuniform. Because the near-wall region is a "power house of vorticity" (Lighthill, 1963), this also then must be nonuniform. Near the point of separation, the fluctuating component of ω_z constitutes almost the entire vorticity because the mean is very small.* Separation occurs instantaneously when the entire local ω_z is lifted away into a hairpin vortex. An example of this is shown in figure 3 where the liftup near the wall coincides

*In a turbulent boundary layer, the hairpin vortex structures are perturbations on the mean flow–their vorticities cannot be derived by differentiating the mean flow velocity profile. However, in other shear flows,as in mixing layers, jets and wakes, the two-dimensional rollups can be derived from the mean velocity profile and therefore are not perturbations on the mean flow (see Gad-el-Hak and Bandyopadhyay, 1994).

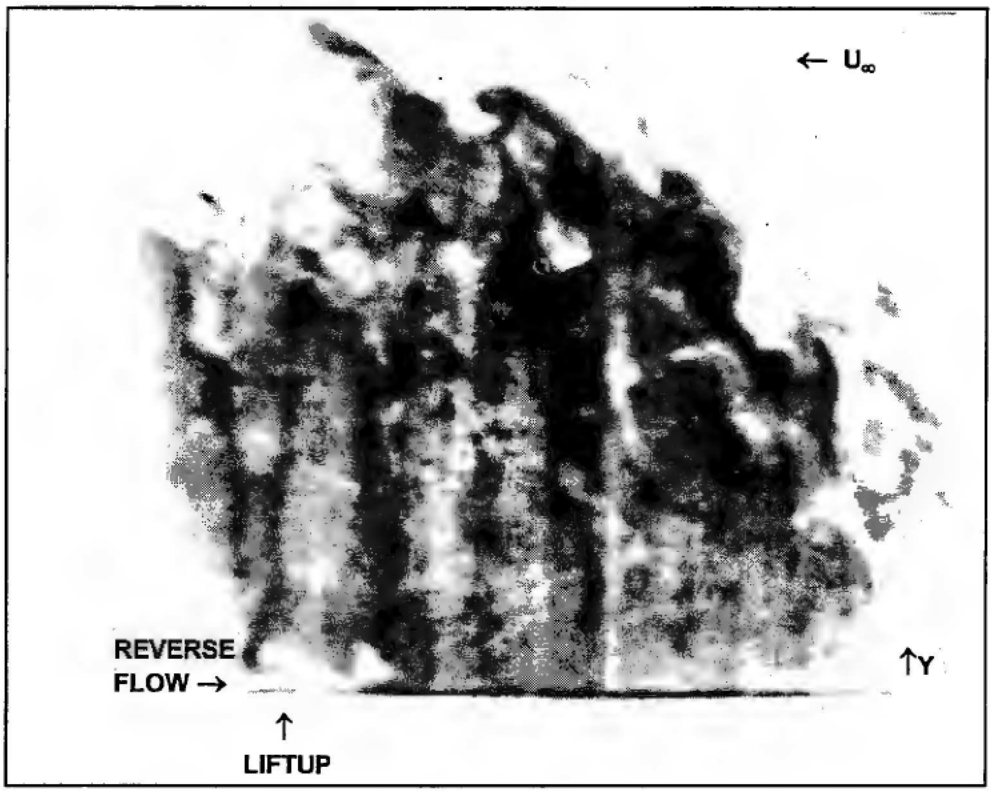

Figure 3. Longitudinal Section Through the Separation Region Showing a Near-Wall Liftup of Vorticity

with separation. Because $w_z \rightarrow 0$ near separation, it follows that separation has to occur at spotty places on the wall at varying times. This is the result of Sandborn and Kline (1961), who observed that incipient separation is an intermittent process.

Simpson (1985) discusses in detail the measurements of the distribution of separation intermittency. (The variable, separation intermittency, is defined in section 6.) It is implicit in the measurements of Simpson et al. (1977) that separation intermittency and the quasi-periodic turbulence production process in a turbulent boundary layer are related. This direction has been further pursued. The following paragraphs describe a hypothesis of the separation process.

In Head and Bandyopadhyay (1981) it has been shown that a large structure is an assemblage of a large number of hairpin vortices, their number per unit-wall area increasing with Reynolds number. While the individual hairpin vortices are ideally inclined at 45° to the flow direction, the envelope of their tips in a large structure generally forms a shallower angle. Head and Bandyopadhyay (1981, p. 307) suggested that as a vortex pair leaves the surface, it induces a velocity in the upstream direction causing a flow deceleration in the immediate vicinity of the wall, and this condition is favorable to the production of a further hairpin. Later on, this hypothesis was firmed up by the long time-averaged, triple-moment measurements of Bandyopadhyay and Watson (1988). They stated that, on average, near the wall of a smooth surface, "shear stress is transported outward and is associated with a deceleration." Such liftup of a hairpin is shown schematically in figures 4(a) and 4(b). This is also arrived at by redrawing Perry and Chong's

(1982) analysis of wall turbulence in the joint context of mainstream and recirculating flows. In figure 3, the liftup consists of smokeless fluid, which represents the recirculating flow of the separated region. The upstream movement of the point of separation at a given span is shown schematically in figure 4(c), where S is also a point of inflection in the wall vorticity distribution. As it happens in a large structure, ideally, the hairpin liftup in figure 4(a) leads to the production of the next hairpin. The process is repeated and a regular large structure forms, but this time, the upstream interface of the large structure coincides with the separation interface (figure 5). This description agrees with the liftups in figures 3 and 4(a) because their sense of vorticity, that is, $-\omega_z$, is the same as in the mainstream. After the large structure has grown to its limit, it is "rapidly" swept downstream, and the cycle is completed. (In the present experiments, because the flow speed near separation was low, it was possible to visually observe the systematic upstream and downstream motions of the point of separation).

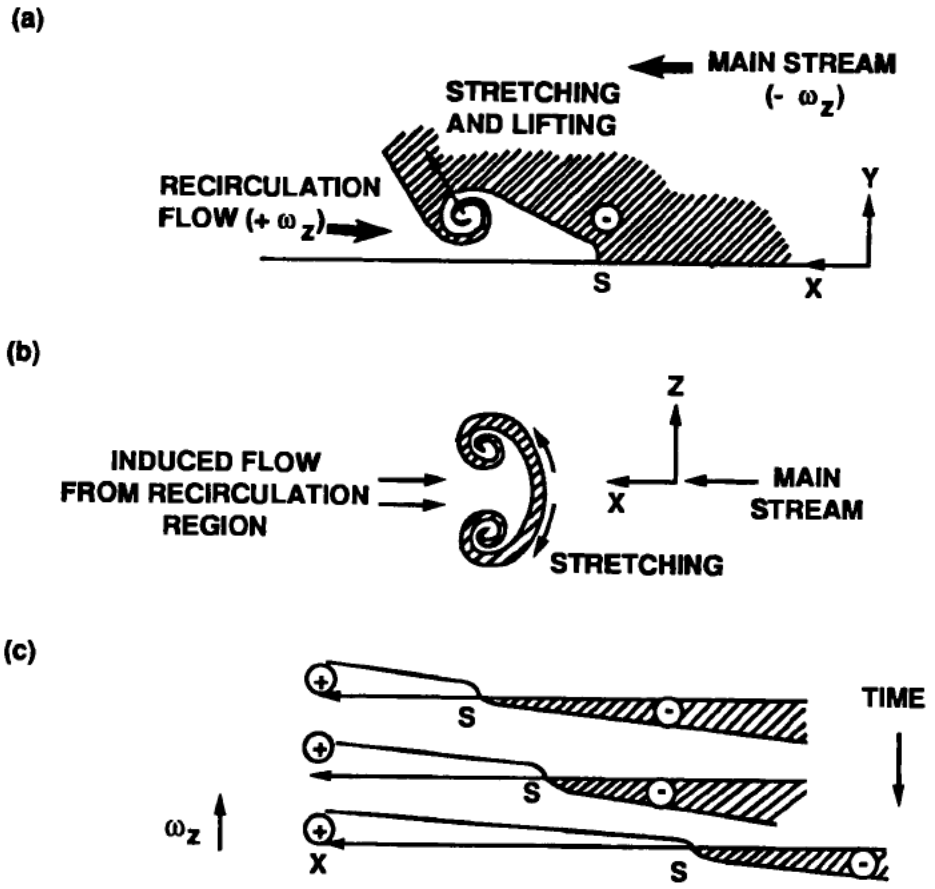

Figure 4. Postulated Dynamics of Separation: (a) Vorticity Liftup at Separation and the Relationship Between Mainstream and Recirculation Regions; (b) Cross-Sectional Plan View at y = Constant in (a) Showing Three-Dimensional Nature of Liftup; and (c) Upstream Propagation of the Point of Separation

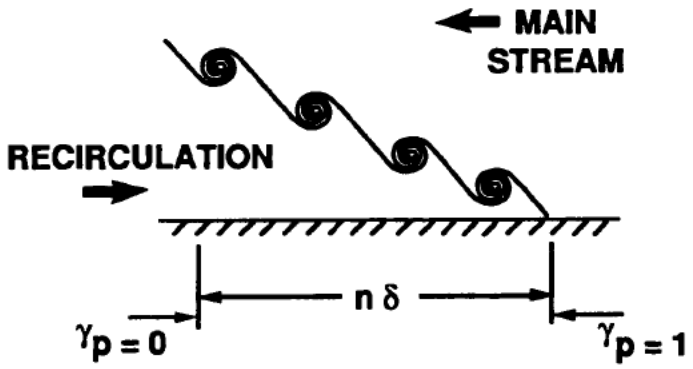

Figure 5. Schematic of the Instantaneous Separation Interface Buried Inside the Boundary Layer During Upstream Advancement of Separation

3. FLOW VISUALIZATION

3.1 BACKGROUND

The turbulent boundary layer, flow visualization experiments were carried out in the Low-Speed Smoke Tunnel of the Cambridge University Engineering Department in the 1970's. But, the visualizations could not be analyzed properly for a long time because the hairpin vortex description of turbulent boundary layers was not sufficiently developed (Head and Bandyopadhyay (1981), Bandyopadhyay and Balasubramanian (1993 and 1994a), and Perry et al. (1991)).

The tunnel is 0.91 m x 0.91 m in cross-section and 12.2 m in length, made of five equal sections. The maximum attainable freestream velocity is 2.5 m/s. The boundary layer is seeded with paraffin smoke and is illuminated with a thin laser-light sheet. Details of the tunnel and the smoke flow visualization technique are given in Fiedler and Head (1966), Bandyopadhyay (1977), and Head and Bandyopadhyay (1981).

The relationship between the smoke-marked and the rotational fields has been discussed elsewhere (Bandyopadhyay, 1977, 1986). More recently, this aspect has been discussed by Fiedler (1988). There, he observed that "...there exists a clear analogy between lines of constant vorticity (isovorts) and streaklines, as long as the viscosity of the fluid remains negligible. This has been discussed by Michalke (1965), who indeed showed perfect identity of streaklines and isovorts in the transition region of a laminar mixing layer" (see figure 8 in Fiedler, 1988). Similarly, in a turbulent mixing layer, Weisbrot and Wygnanski (1988) have shown that both the streakline pattern and isovorts resemble the ensemble superposed smoke pictures very well.

3.2 ADVERSE PRESSURE GRADIENT EXPERIMENTS

Figure 6 shows the arrangement used to produce a strong, localized adverse pressure gradient. Only the first three of the five tunnel sections were used. The roof of the third section was tilted up to vent off part of the flow, and a perforated metal screen was mounted across the exit of the section. In addition, 19 cm of this screen near the floor was completely blocked off to increase the severity of the pressure gradient. The boundary layer was found to undergo an incipient separation near the exit when the stream velocity in the far upstream zero pressure gradient region was 1.5 m/s. This blockage height of 19 cm was arrived at gradually and represents the minimum height required to produce an intermittent separation (see figures 7 through 9 and 12). It was argued that in such a gradual onset of separation, the recirculation region offers the least disturbance to the upstream turbulent boundary layer under investigation. Smoke injection into the boundary layer developing on the floor revealed that there was only a mild flow from this boundary layer up along the side walls, and cross-stream illumination showed that the major part of the flow along the floor was substantially uniform.

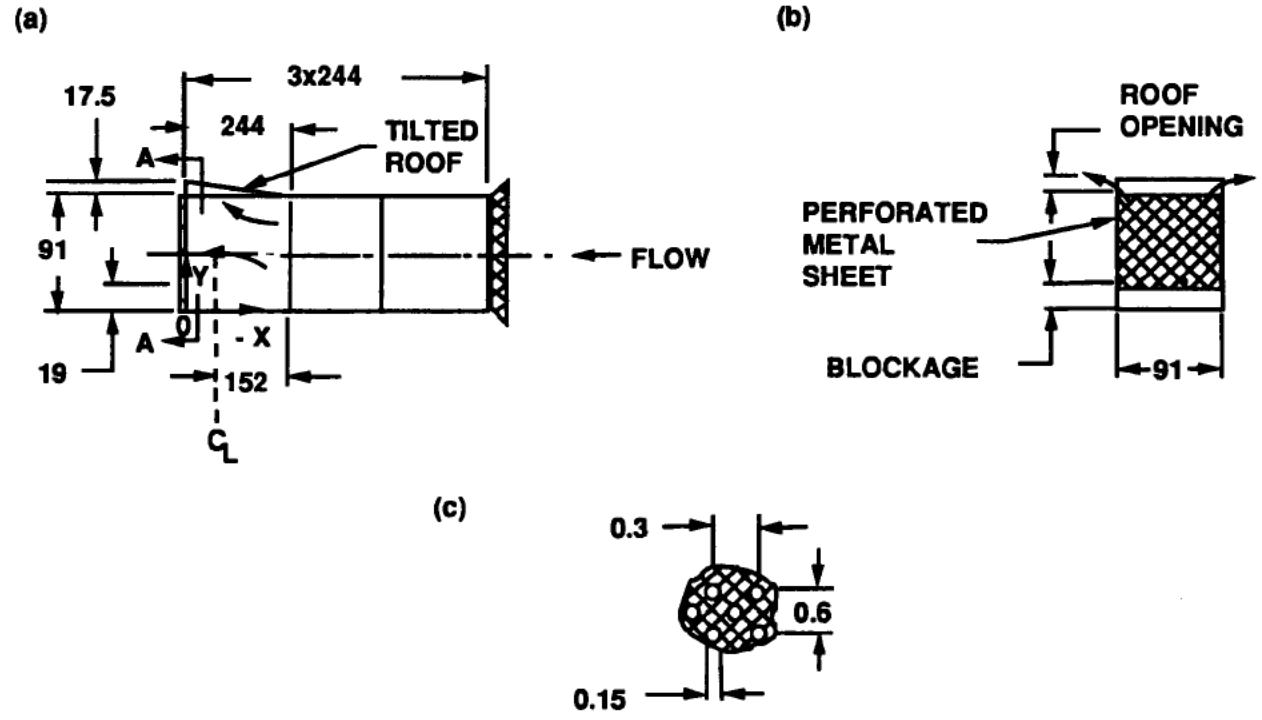

Figure 6. Tunnel Arrangement Used to Produce Adverse Pressure Gradient: (a) Longitudinal View; (b) End View AA Marked in (a);and (c) Perforated Metal Sheet Details (Dimensions are in cm.)

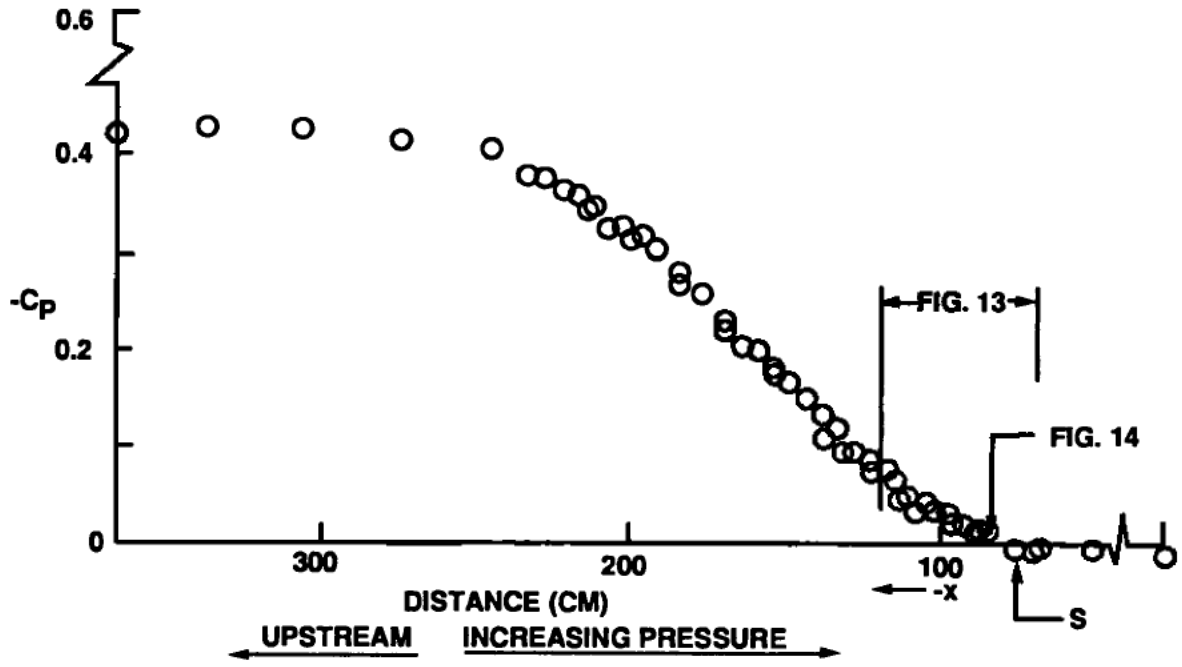

Figure 7. Longitudinal Surface-Pressure Distribution Measurements Along Centerline of the Tunnel Floor in Adverse Pressure Gradient Experiment

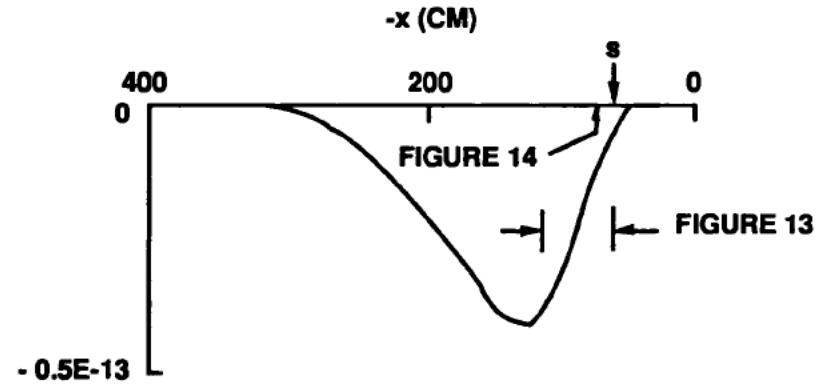

Figure 8. Pressure Gradient Parameter in the Adverse Pressure Gradient Experiment (Ordinate Is Proportional to K; Mean Separation Location Is Indicated by S)

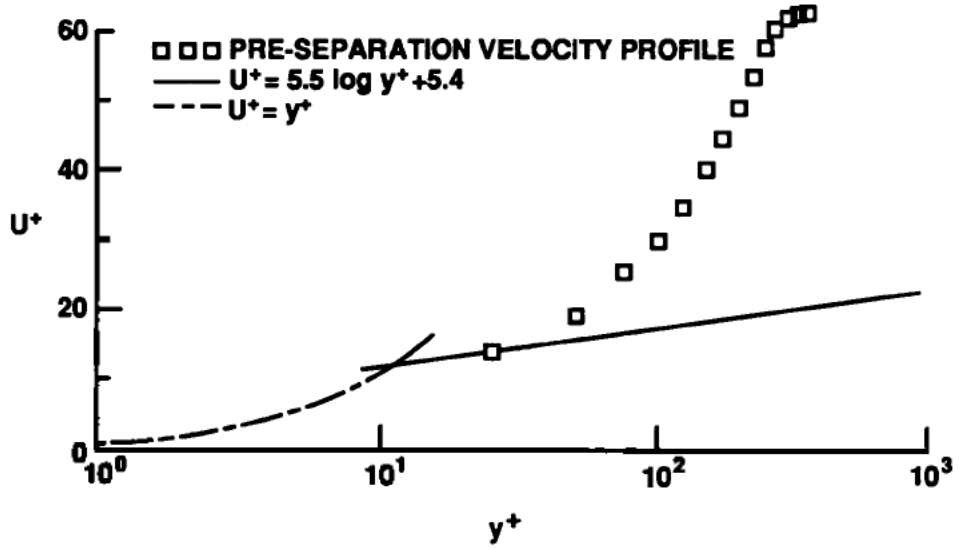

Figure 9. Measurements of Pre-Separation Velocity Profile Plotted in the Law of the Wall Coordinates

Reverse Blank

4. MEASUREMENTS AND COMPUTATIONS

4.1 LONGITUDINAL SURFACE PRESSURE DISTRIBUTIONS

The longitudinal surface static pressure distribution along the floor was measured with a static tube (3.5-m length, 6-mm diameter) traversed along the tunnel midplane. The nose of the static tube was elliptically rounded, and the static holes were circumferentially located 16.5 cm from the tip. The pressure differentials with respect to the reference were measured with an inclined-tube alcohol manometer (15 cm long) at inclinations of about 5°. These measurements are accurate to within 1 percent. The pressure distribution is shown in figure 7. Here, the coefficient of pressure c_p is defined as $(p_r - p)/q_r$ where p_r and q_r are the far upstream (x = -350 cm) reference static pressure and dynamic head, respectively. The data include repeated runs. Locations where longitudinal and cross-stream sections of the smoke-filled boundary layer were photographed with a 35-mm camera are indicated in these figures. The mean location of the visually observed onset of intermittent separation is indicated in figure 7 by the symbol S.

Boundary-layer computations were carried out using the measured pressure distribution. The streamwise distribution of a scaled version of the pressure gradient parameter K is given in figure 8. The locations where the longitudinal and cross-stream pictures were taken are marked therein. Because the tunnel blockage was set for the least-needed gradient for a separation to occur, the visually observed location of intermittent separation should be very close to where

$$K = (\nu / U_\infty^2)(dU_\infty / dx) = 0;$$

figure 8 shows this indeed is the case.

Currently, it is not possible to accurately compute separating turbulent boundary layers in the neighborhood of separation. The relevance of the effects of the pressure gradient on the hairpin vortices to the terms in a conventional boundary-layer computation can be seen in so-called lag constants of turbulence closure models, or by examining the x-derivative of the pressure gradient parameter K,

$$\frac{dK}{dx} = -2\left(\frac{dU_\infty}{dx}\right)^2\left(\frac{\nu}{U_\infty^3}\right) + \left(\frac{\nu}{U_\infty^2}\right)\left(\frac{d^2U_\infty}{dx^2}\right). \tag{3}$$

Because the sign of dK/dx is determined by the acceleration derivative only, which directly affects vortex stretching and rotation, the pressure gradient can be expected to have two regions of characteristic turbulence depending on whether dK/dx is positive or negative. In figure 8, these two regions extend roughly over 120 cm < -x < 50 cm and 320 cm < -x < 120 cm. Although the rate of application of the pressure gradient is not normally taken into account, for accurate turbulence modeling, it should be. This observation could be useful because predicting the mean point of separation accurately is difficult even today (see figure 12).

4.2 BOUNDARY-LAYER MEASUREMENTS

The boundary-layer mean velocity profiles were measured to determine the conditions at which the flow visualizations were performed. In the low-speed smoke tunnel, the boundary layer was tripped by a saw-toothed trip, and the measurements were conducted at about 6 m downstream. The mean velocity profiles were measured by flattened and rounded traversing Pitot tubes. The very low dynamic pressures were measured both by an inclined-tube alcohol manometer (15 cm long) at inclinations of approximately 5°, and a sensitive weighing manometer (Head and Bandyopadhyay, 1981). Small but systematic variations between mean velocity profile measurements were observed because of the low dynamic heads. At least three profiles were measured at the same condition; those presented in this report are the averages.

The mean velocity profiles through the experimental points were enlarged and manually digitized at closer spacings than the experimental points, and from those, the values of shape factor H and the momentum thickness Reynolds number Re_θ were calculated. These values agreed within 2 percent with those calculated from fittings of power-law velocity profiles.

The coefficient of local skin friction c_f was determined using the Clauser plot ($c_f = 0.00055$), the Ludwieg-Tillmann relationship (= 0.000566), and the new skin-friction law of Head (= 0.00054), which uses the measured values of H and Re_θ (figure 4.1(x) of Head (1968)).

The mean velocity distribution across the boundary layer was measured on the floor centerline just upstream of separation. These measurements are accurate to within 1 percent. The profile is shown in the wall-layer coordinates in figure 9. It is known in a layer approaching separation (unlike that in a relaminarizing turbulent boundary layer) the extent of the log region diminishes gradually and not abruptly. A log region is barely present, as to be expected, in figure 9. Because virtually all adverse gradient velocities are beyond the log layer, the measurements are compared with Thompson's (1965) profile in figure 10. The slight discrepancy is attributed to errors in the measured values of H and Re_θ arising from the difficulties in measuring very low dynamic heads (<1.5 m/s). A somewhat higher value of H, or lower value of Re_θ, or both would give a better agreement.

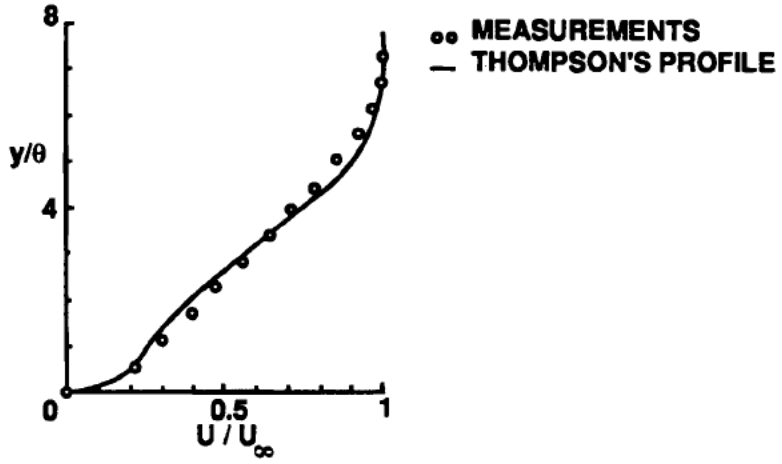

Figure 10. Mean Velocity Profile Measurements Prior to Separation Compared with Thompson's (1965) Profile

At the flow visualization station, if the pressure gradient was zero, the boundary-layer integral quantities H, c_f, Re_θ, and δ would be 1.426, 0.0042, 1170, and 12 cm, respectively, at a free-stream velocity of 1.5 m/s. When the same flow is subjected to an adverse pressure gradient just ahead of the region of incipient separation, H, c_f, Re_θ, and δ reach values of 2.529, 0.000545, 2880, and 24 cm, respectively. In all pressure gradients, the value of H correctly describes the characteristics of intermittency, which is intimately tied to entrainment (Fiedler and Head, 1966).

The measured boundary-layer integral quantities in the separation experiment are compared with other authors' measurements in figure 11. The present experiment agrees with the separation trajectory of Perry and Schofield (1973) and the measurement of Simpson et al. (1977). Figure 11 shows that the visually determined fact—a spatially intermittent separation is taking place in the present experiment—agrees with similar observations of Sandborn and Kline (1961) in similar conditions. The freestream u and v turbulence levels, respectively, were 0.21 and 0.15 percent of the freestream velocity. These measurements show that the tunnel floor boundary layer is behaving as is expected of a flat-plate, turbulent boundary layer.

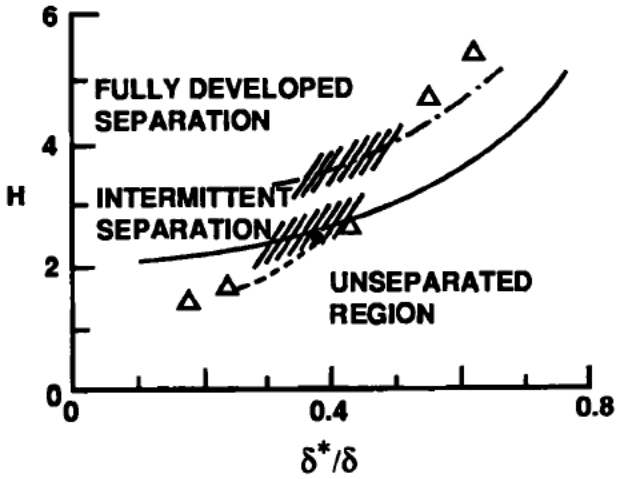

Figure 11. Comparison of Present Separation Experiment (Filled Circle) with Plots of Simpson et al. (1977) (Broken line is Perry and Schofield's (1973) separation trajectory; triangle is Simpson et al.(1977); hatched region is from Sandborn and Kline (1961); solid and chain lines are from Sandborn and Kline.)

4.3 BOUNDARY-LAYER COMPUTATIONS

In turbulent boundary layers subjected to pressure gradients, the mean location of the rotational/irrotational outer layer and its spread, as given by the standard deviation, are known to be related to the form parameter H of the mean velocity profile (Fiedler and Head, 1966). (Here, H is defined as the ratio of the boundary-layer displacement thickness to the momentum thickness.) Furthermore, the aspect ratio of the constituent vortices in a zero pressure gradient boundary layer depend on the momentum thickness Reynolds number Re_θ (Head and Bandyopadhyay, 1981). These quantities are expected to vary greatly as the point of separation is approached. The development of the boundary layer was therefore computed to obtain the complete streamwise distributions of H, c_f, Re_θ and δ because unfortunately they were only measured very near the mean point of separation. Because separation turbulence is difficult to model, it was also hoped that a qualitative comparison of the structures with the mean computations might shed some light on what are known as lag effects in turbulence modeling.

4.3.1 Method

The two-dimensional turbulent boundary-layer equations were solved using an implicit finite difference procedure and a mixing length turbulence model, the details of which are given elsewhere (Bandyopadhyay, 1989b). The computations were carried out at the National Aeronautics and Space Administration Langley Research Center. To account for the laminar-to-turbulent transition process, the computations were matched to the measurements of momentum thickness in the far upstream zero pressure gradient region. The measured pressure distributions shown in figure 7 were smoothed and used in the computations. (Note that in the figures describing the experiments, the origin of the streamwise distance x is taken at the tunnel exit of the third tunnel section, and it is negative in the streamwise direction.) In an adverse pressure gradient flow leading to separation, it is known that the region of backflow causes the actual pressure gradient to be different from that calculated from inviscid considerations alone. Therefore, the fact that the present adverse pressure gradient computations use the measured pressure values should make the computations realistic.

The work of Glowacki and Chi (1972) and Galbraith and Head (1975) show that adverse pressure gradient affects the slope of the mixing length near the wall ℓ. Defining the pressure gradient parameter as

$$\beta = \left(\frac{\delta^*}{\tau_w}\right)\left(\frac{dp_w}{dx}\right),$$

the following relationship given by Glowacki and Chi (1972) was used for $\beta \geq 0$,

$$\ell = 0.41 + 0.182[1 - \exp(-0.321\beta)]. \tag{4}$$

In the adverse pressure gradient boundary layer, neither lag nor any other effects were considered. Thus, the modeling in the pressure gradient flow is free from any arbitrary constant.

4.3.2 Results

The computed distributions of the boundary-layer integral quantities and δ are shown in figure 12.The following limited statements on the uncertainties in figure 12 may be made. While the numerical results presented are insensitive to grid resolution, the turbulence closure model significantly underpredicts the integral quantities near separation. The error in the model is much larger than that in the measurements. This modeling error is attributed to the lack of understanding of the separation process.

As far as the location of the mean point of separation is concerned, the wall-shear stress plot shows that the visual observation is consistent with the measurement and computations. (A consistency check was also offered by figure 11.) The values of δ are included because it is a meaningful quantity as far as the distribution of the outer layer intermittency of the rotational/ irrotational interface is concerned. This figure can be compared with the measurements of Schubauer and Klebanoff in a separating airfoil (flow 2100) and the computations according to the method of Bradshaw, Ferriss, and Atwell, as well as a simplified version of it (see figure 11 of Patel and Head, 1970). The trends are identical. The computed wall-shear distribution indicates that the present computations are probably accurate ahead of the region of separation extending over an x-value of at least 50 cm, and the inaccuracy spreads over twice as much in the airfoils.

In the airfoils, three-dimensional effects and surface curvature effects do not significantly account for the disagreement between measurements and computations, leading Patel and Head (1970) to comment that "there is a possibility that there may be other important effects which come into play near separation." What are these effects? Near separation, there are three unique characteristics that have not been exclusively accounted for in the models: (1) the upstream effect of the downstream recirculating flow (this is the diffusion effect, not the mean pressure gradient effect, which has already been considered in the present numerical computations); (2) the intermittent nature of the separation process near the wall (Sandborn and Kline, 1961); (see also Simpson, 1985); and (3) the rapid vortex stretching taking place near separation. Note that these effects are largely absent in a non-separating boundary layer on which the presently used equation (4) is based.

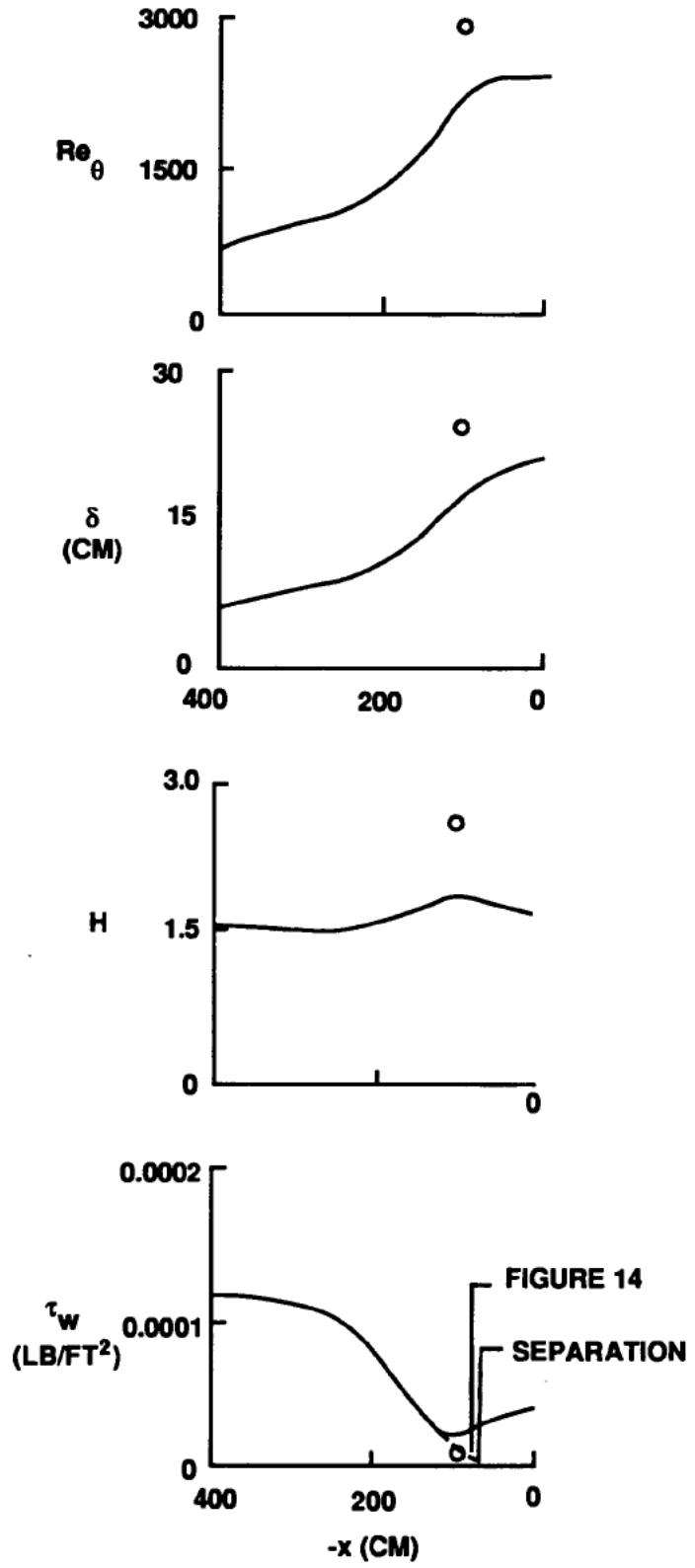

Figure 12. Computed Developments of Adverse Pressure Gradient Boundary Layer (Solid Lines) and Measurements (Symbols) at Pre-Separation Station

5. RESULTS FROM VISUALIZATION EXPERIMENTS

The visualization of several longitudinal sections through the region of separation is shown in figure 13. The two regions of interest are the separation interface attached to the wall, which is also buried in the boundary layer (figure 5), and the rotational interface with the freestream (figure 2). The point of separation moves upstream and downstream in a quasi-cyclical fashion. When separation has advanced upstream, the upstream interface slope of the separated region (figure 5) varies between 20° and 40°. The interface is approximately linear and contains spiraling rollups reminiscent of large structures in a zero pressure gradient turbulent boundary layer (Head and Bandyopadhyay, 1981). The size of these rollups are known to be Reynolds number-dependent. Near the region of separation, $Re_\theta = 3 \times 10^3$ (figure 12).

There are two notable points about the spirals in the separation interface. First, the spiraling eddy is order of magnitude smaller than the local δ as is characteristic of higher Reynolds number turbulent boundary layers (Head and Bandyopadhyay, 1981) (compared to the far upstream zero pressure gradient boundary layer at $Re_\theta = 10^3$). Secondly, the streamwise spacing between the eddies is much larger than what it is in zero pressure gradient flows at $Re_\theta > 10^3$ and $H < 1.4$ (Head and Bandyopadhyay, 1981). The reason for the latter is probably that there is less vorticity at the wall available near separation to rollup. The separation interface, which is marked by the smoke/non-smoke boundary, is also the upstream interface of the last large structure of the main stream as was argued earlier. It should be noted that the similarity of these separation large structures to those in a canonical flat-plate, zero pressure gradient boundary layer is qualitative.

In the outer layer, where the flow is intermittently rotational and irrotational, the outer layer smoke filaments in figure 13 show that, in the neighborhood of separation, the linear features are approaching an upright posture ($\alpha \rightarrow 90°$). The longitudinal sections show that the boundary layer begins to thicken rapidly *just prior to separation* (in x-distances 0 (δ)) and much after the application of the adverse gradient (figures 7 and 8). From experience, the visual impression is that, in comparison to that in a zero pressure gradient flow (Head and Bandyopadhyay, 1981), near the freestream, the upstream rotational/irrotational interface is crowded with small-scale motions, and they are relatively smaller in scale.

The cross-stream sections just prior to separation are shown in figure 14. The spatially defined outer-layer intermittency function, measured from the cross-stream pictures, is close to Fiedler and Head's (1966) temporally measured function with an optical probe at values of $H = 2.46$ (see their figure 13). The outer rotational/irrotational intermittent layer extends over $0.7 > y/\delta > 1.2$. This spread of intermittency is much narrower than that in free wakes and jets. In comparison to those in low Reynolds number (Re_θ), zero and favorable pressure gradient turbulent boundary layers, the present adverse gradient flow has a thicker turbulent core (Head and Bandyopadhyay (1981) and Bandyopadhyay (1989a)). This is in agreement with Fiedler and Head's suggestion. The interface shape in figure 14 is noticeably different from that in zero and favorable pressure gradient flows (Bandyopadhyay, 1989a) as well as free wakes and jets. It consists of large (in absolute size) upright bulges with *fewer foldings*.

Figure 13. Longitudinal Sections Through the Smoke-Filled Intermittently Separating Turbulent Boundary Layer

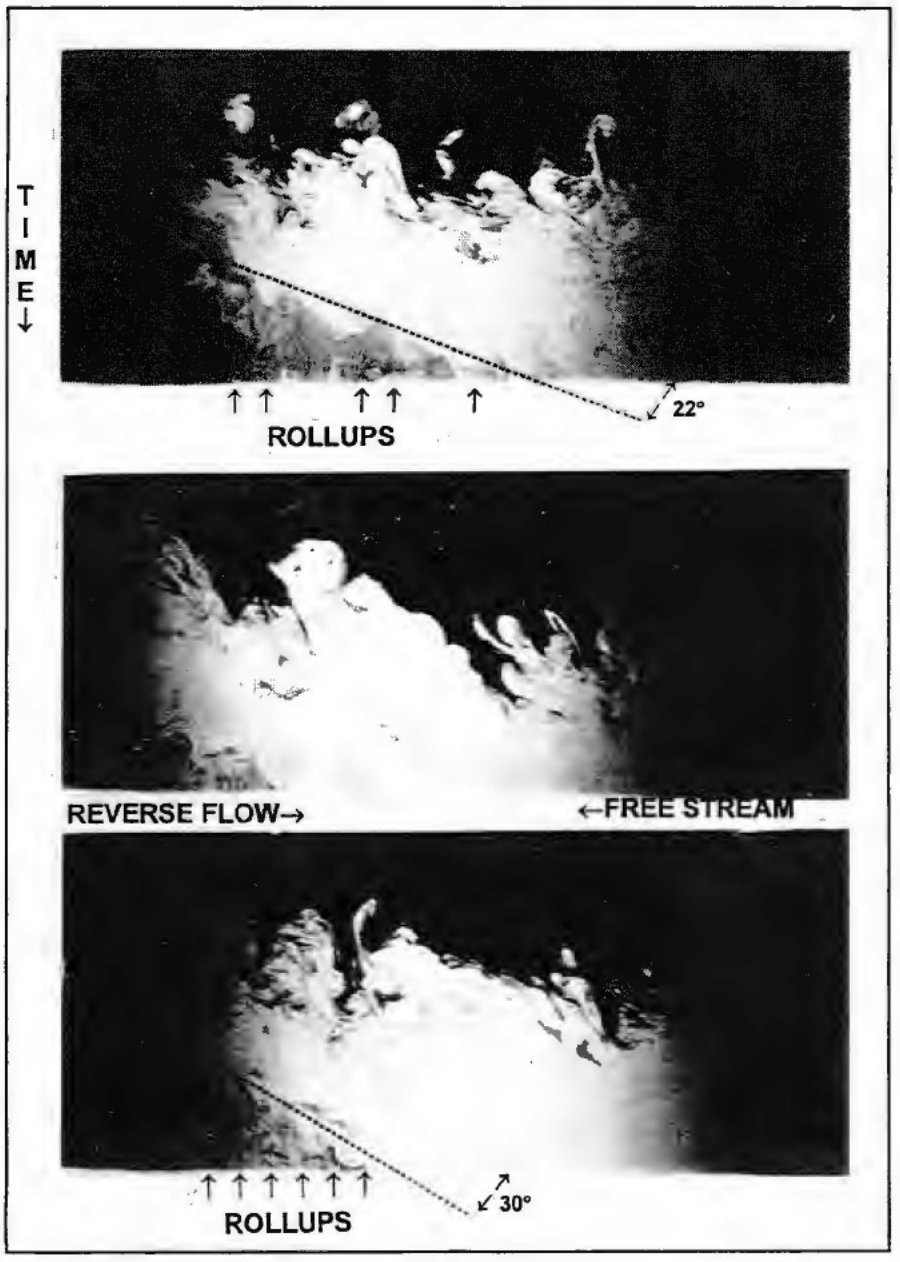

Figure 13. Longitudinal Sections Through the Smoke-Filled Intermittently Separating Turbulent Boundary Layer (Cont'd)

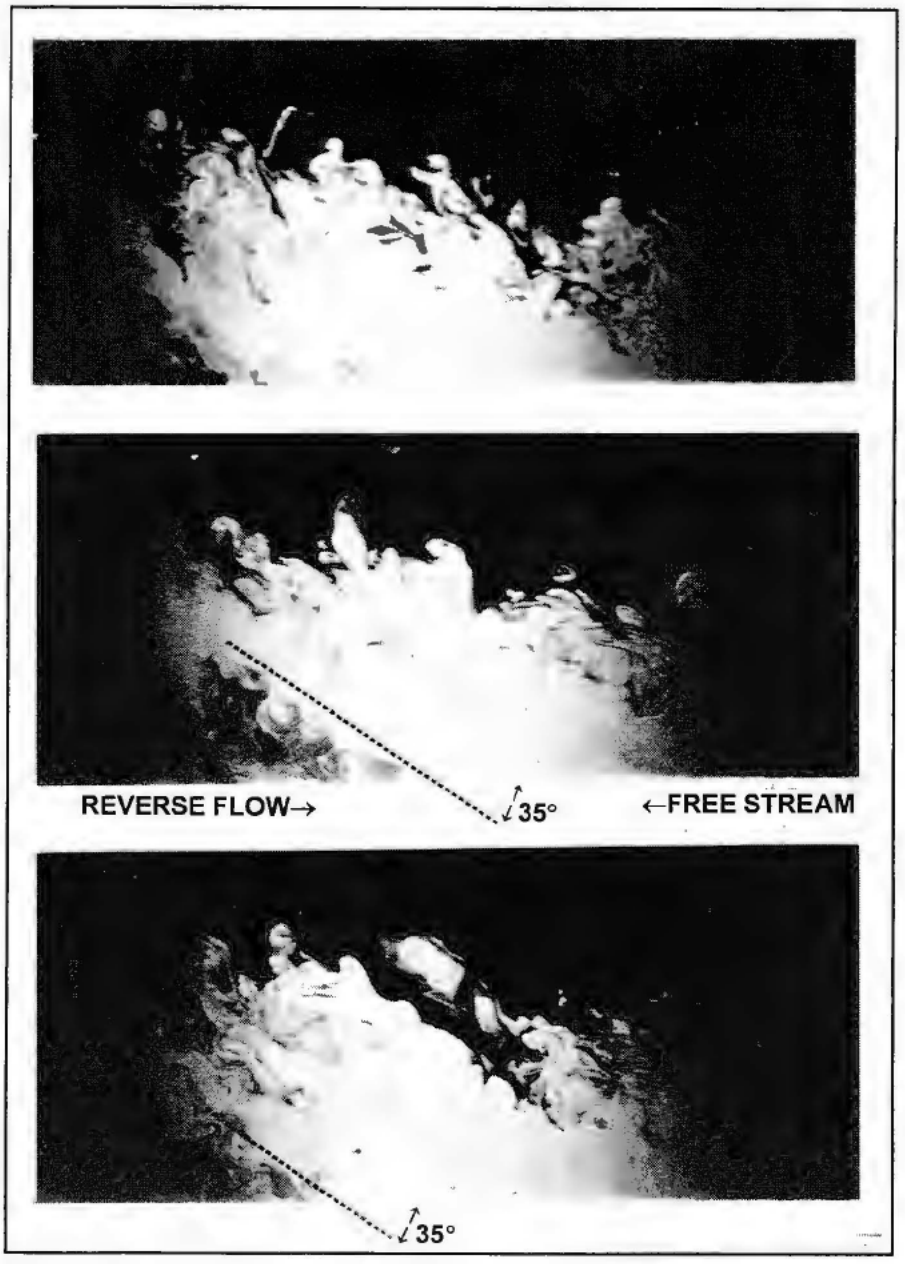

Figure 13. Longitudinal Sections Through the Smoke-Filled Intermittently Separating Turbulent Boundary Layer (Cont'd)

Figure 14. Cross-Stream Views of the Smoke-Filled Adverse Pressure Gradient Boundary Layer Just Prior to Separation

6. A LOW-DIMENSIONAL STRUCTURAL MODEL OF SEPARATION INTERMITTENCY

The observations on the phenomenon of incipient separation are used in the following section to develop a low-dimensional structural model for calculating separation intermittency. To a standing observer, the separation process appears as a ramp-like time series—the upstream advancement being more gradual. It is assumed that, simultaneously, the point of separation moves spanwise, with the hairpin vortices forming in a "domino"manner, although, this is not strictly needed in the model. The region of separation is shown schematically in figure 15(a). After the large structure has reached its maximum length (see below), the point of separation moves rapidly downstream, and the cycle is completed. The justification for a domino-like breakdown comes from three sources. First, Perry et al. (1981) have shown that this is how a turbulence spot grows. Second, several longitudinal and spanwise spacings between hairpin vortices relevant to the domino effect are also present in a fully turbulent boundary layer (Bandyopadhyay, 1983). In a flat plate having an unlimited span and length, in the course of time, the overall arrowhead shape of a turbulence spot would still be recognizable, but deep inside the spot, the layer would look like a turbulent boundary layer whose Reynolds number is increasing. So, the domino-like spread should be qualitatively expected to occur in a fully turbulent boundary layer also, including when there is a pressure gradient. Finally, this assumption receives some support from Simpson et al. (1977, p. 575) whose pre-separation, long time-averaged, spanwise, correlation measurements have "revealed a distinct periodic behavior superimposed on a larger-scale decay of the correlation."

Assume that the upstream propagation speed of separation is constant. The time during which the flow is separated at any point along the centerline is then given by a triangle as shown in figure 15(b). The intermittency distribution is, therefore, simply the result of a summation over many similar triangular times whose distribution is seemingly random. The spanwise jitter is ignored in figure 15(a) because the triangles are similar and only the centerline needs to be considered.

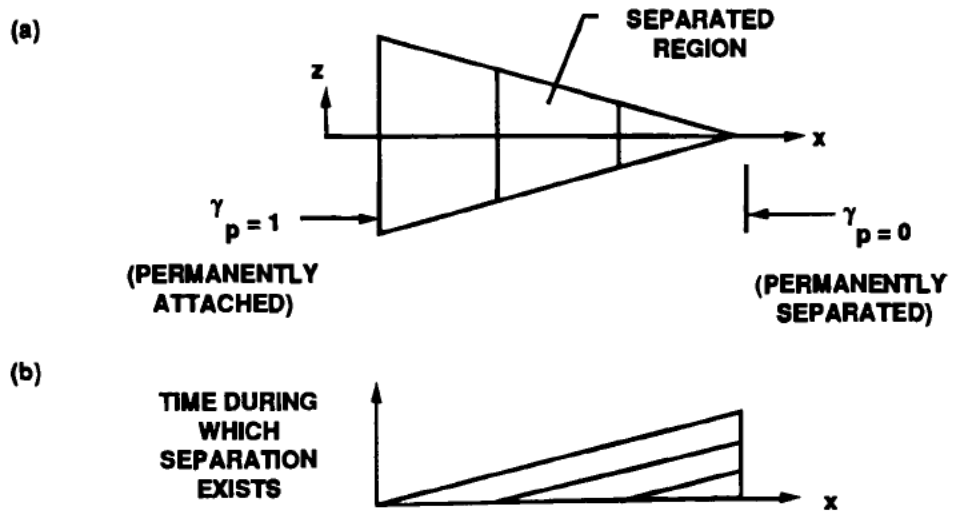

Figure 15. Schematic of (a) Plan View of the Domino-Like Upstream and Spanwise Propagation of the Point of Separation; (b) Times During Which Separation Exists at (x, 0, z)

To calculate the intermittency distribution accurately, the length distribution of the large structures is required. This situation is one in which a statistical approach, implying that the phenomenon is random in nature, would be commonly prescribed. This author proposes that this assumption is not justified because of the quasi-organized dynamics. The dynamics in this research was modeled after Van Maanen (1980), who conducted an experiment in a pipe-flow apparatus with laser Doppler anemometry on the organized eruptions very near the wall. Van Maanen stated that "the measurements of the time interval distribution shows a very wide distribution which is close to linear on a semi-logarithmic scale. This suggests a certain underlying mechanism that we do not yet know. But it is too typical to be accidental." He added that "the velocity signals show the phenomenon is accompanied by strong vortex motions." In the following, it is hypothesized that this semi-logarithmic distribution applies to the streamwise size of the large structures also, and the underlying mechanism is essentially low-dimensional in nature, whereby the concepts of chaos theory are applicable.

Because a large structure is an assemblage of hairpin vortices, it is assumed that the train of large structures is also organized and their sequential size distribution is actually amonotonic, but not random, thus explaining why it seems to be random. These tasks remain to be done: (1) establishing the relationship that determines the size of a large structure and (2) determining how to incorporate that relationship mathematically so that a chain of generations is created. As Van Maanen (1980) did with burst time intervals, it is assumed that requirement (1) is given by the exponential relationship

$$\phi = e^{-\psi}, \tag{5}$$

where ϕ is output and ψ is input. For requirement (2) it is assumed that the length of a given large structure is determined only by that of the immediately preceding one. (This is similar to the earlier statement that a lifting hairpin vortex has to create the retarded flow condition near the wall that is necessary for the formation of the next hairpin.) The lengths of the large structures in a train will sequentially be

$$\phi,\ \exp(-\phi),\ \exp[-\exp(-\phi)],\ \exp\{-\exp[-\exp(-\phi)]\},\ \ldots, \tag{6}$$

and so on. After normalizing x-distances by the length between the fully separated and fully attached regions, that is, by stating that the length of the largest large structure (ϕ) is 1, the successive lengths turn out to be

$$0.368,\ 0.692,\ 0.500,\ 0.606,\ 0.545,\ 0.58,\ 0.560,\ 0.571,\ 0.565,\ \ldots. \tag{7}$$

For $\phi = 2$, the lengths are

0.135, 0.873, 0.417, 0.659, 0.518, 0.596, 0.551, 0.576, 0.562,
0.570, 0.565, 0.568, 0.567, 0.567, 0.567, 0.567, ... (8)

Similarly, for other values of ϕ, after some oscillations, the lengths settle down in the neighborhood of 0.567. Figure 16 shows equation (5) and a map of its regular attractor-like behavior for $\phi = 1$. From this point of view, the mean is actually the limiting value of the generational propagation rather than simply a statistical quantity that has no regard for the underlying physics.

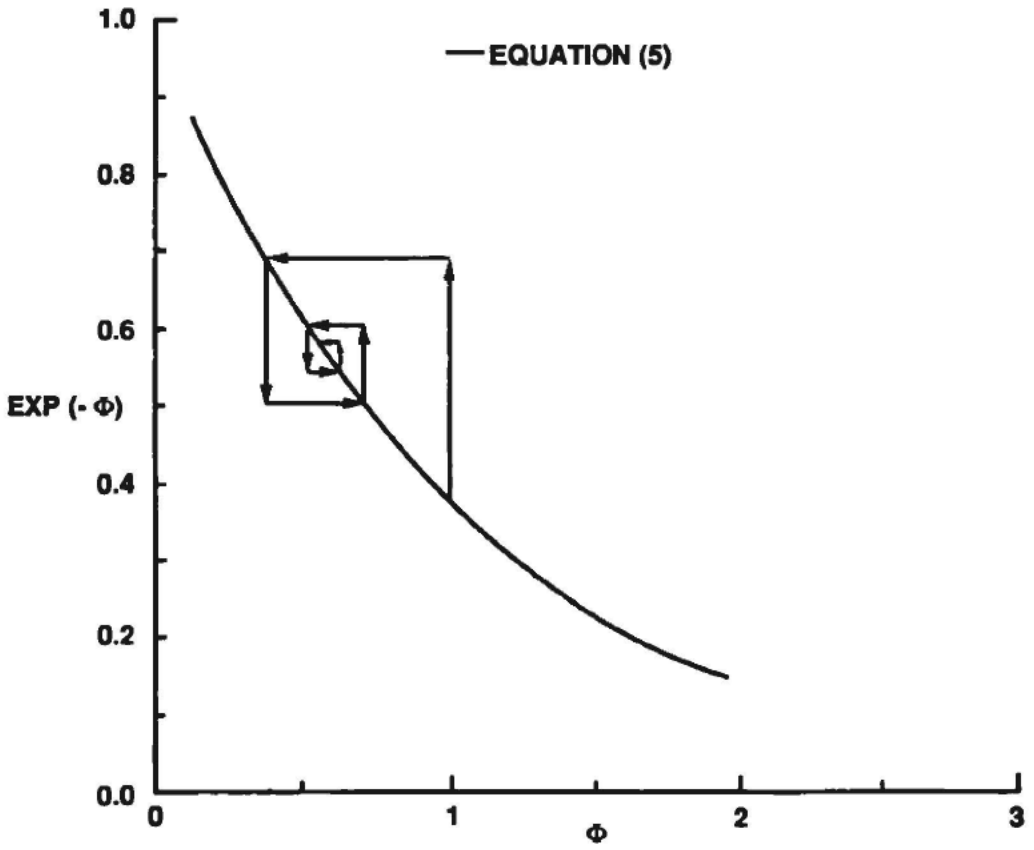

Figure 16. Regular Attractor of the Proposed Model of the Separation Process

Defining intermittency γ_p as the fraction of time the flow very near the wall $(y \to 0)$ is in the downstream direction, its streamwise variation with only 1, 2, 3, or 4 large structures is then as given in figure 17(a). The distributions in figure 17(a) were obtained by summing the times during which separation exists at a given x (figure 15(b)) and then normalizing it. Finally, in figure 17(b), the theoretical γ_p distribution for $\phi = 1$, is compared with the measurements of Simpson et al. (1977) by matching only their streamwise distance over which γ_p effectively varies from 0 to 1. The agreement is good. It is interesting that only the first four large structures, specifically, 0.37, 0.69, 0.50, and 0.61, are adequate to broadly describe the intermittency distribution; the remaining large structures merely make the distribution smoother.

With descending generations, the lengths in equations (7) and (8) vary less between the generations; that is, they begin to look alike. Consider a parallel characteristic of turbulent shear flows in general. Corrsin (1957) has pointed out that the eddy viscosity (ν_T)-based Reynolds number of fully turbulent jets and wakes is constant and is similar to the corresponding critical Reynolds number of their laminar counterpart. Echoing that, Townsend (1970) has postulated how eddy viscosity is maintained at the appropriate level in such flows: ν_T first decays, creating an instability that results in an abrupt increase in entrainment, which increases ν_T, which then decays, and so on. Thus, in the present model, the distributions (equations (7) and (8)) might be considered to pertain to one cycle of instability. As the length becomes asymptotic, conditions become opportune for a new instability wave to set in. These concepts are similar to the surface renewal theories of Black (1968) and others. What is being implied is that, by and large, only one cycle of the instability wave or the incipient separation is adequate to describe the measurements of separation intermittency and, perhaps, its control.

The proposed model departs from the current understanding of intermittency, which is statistical. The concept of generational propagation (equation (5)) has been a key to this development. Measurements are needed to verify the assumptions; the present model has a few scenarios that are at least well-posed, and, based on them, new experiments can be designed for exploring the structural nature of the separation phenomenon, as well as its control. The region of intermittent separation is so well defined in space (in contrast to a region of turbulence production in an attached and regular turbulent boundary layer) that it allows the unique opportunity o investigate the dynamic aspects of hairpin liftups from the wall, large structures, and the domino-like propagation of the liftup process in a controlled manner.

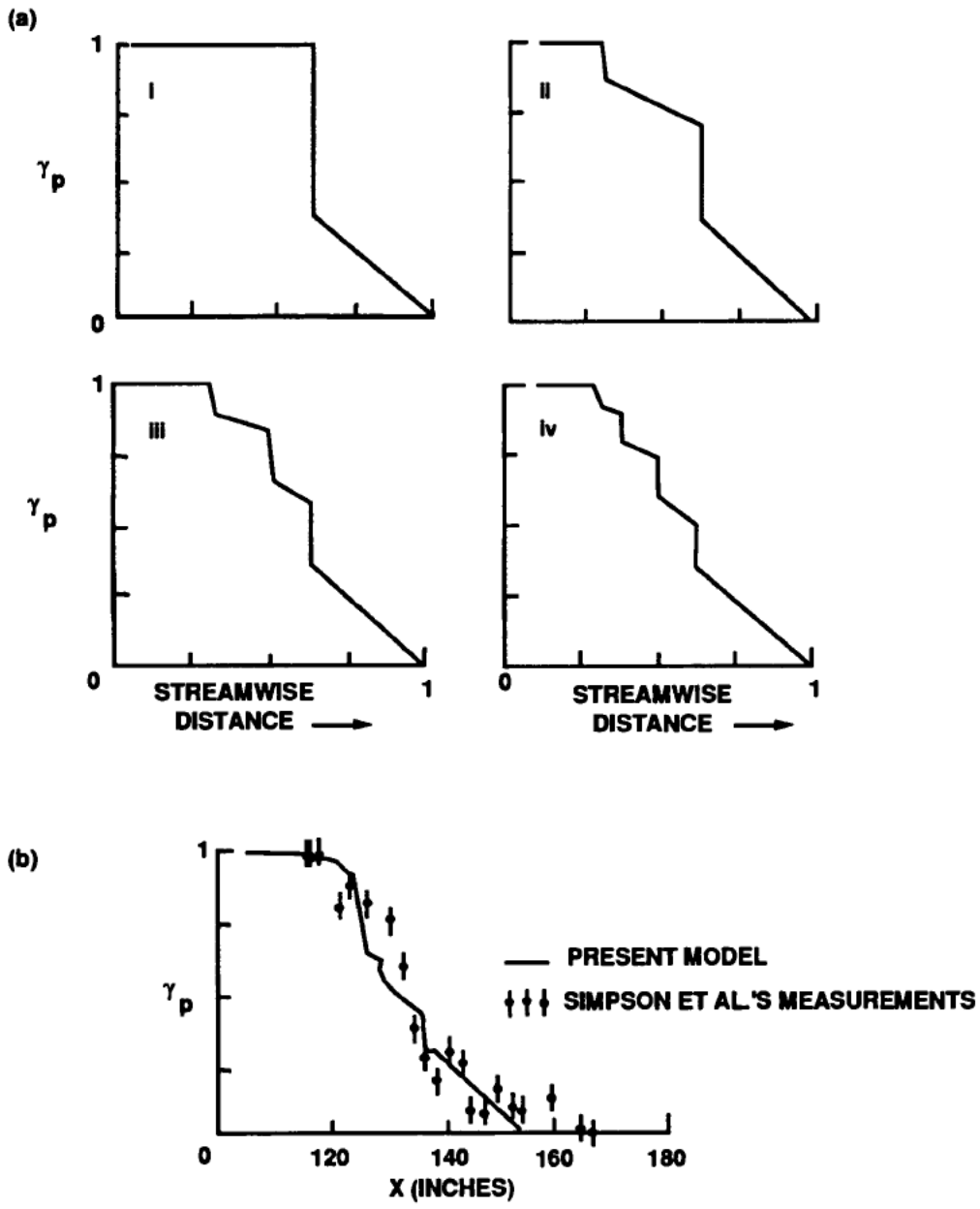

Figure 17. Separation Intermittency Based on Proposed Model: (a)Streamwise Variation of γ_p with a Train of 1, 2, 3, or 4 Successive Large Structures in (i) to (iv) respectively; (b) Comparison of Present Model with Measurements of Simpson et. al. (1977)

7. RELEVANCE TO CHAOS THEORY

The most important significance of the proposed structural model is that there is a sequence of large structures involved in the separation process and that this sequence has a regular attractor. This description is compatible with the classical intermittent breakdown mechanisms in turbulent shear flows proposed by Corrsin (1957) and Townsend (1970), among others. The work shows how the features of hydrodynamics, in general, and the intermittent separation process, in particular, can be treated within the framework of nonlinear dynamics/chaos theory.

It is not clear whether the sequence of large structures proposed is special to the separation process, and it is irrelevant to a canonical zero pressure gradient turbulent boundary layer. But such a possibility remains. Near the region of separation, a consequence of the compression of the irrotational patches marked in figure 2 would be that, because of a newly found proximity, the rotational patches would have an opportunity to organize each other per Biot-Savart law. A mutual induction effect, which would be a powerful self-organizing mechanism, would be setup near the region of separation. This procedure is similar to the organizing effects that an external excitation is known to impose on a turbulent shear layer. It is widely believed that in an open system (that is, in a flow field that has an unbounded freestream), the dimension of turbulence can be low only if the flow is excited. The present work implies that the inherent mutual induction near the region of separation leads to self-organization and this is, in effect, such an exciting mechanism. Therefore, the applicability of chaos theory to an open system of intermittently separating turbulent boundary layer is not unreasonable.

Theoretical efforts have been largely directed towards the development of predictive tools in the design of aerodynamic or hydrodynamic vehicles or components. Various turbulence closure models are examples of that. Structural models are a new development. Although there has been some success in calculating the properties of a turbulent boundary layer, like the root mean square values of wall-pressure fluctuations (Bandyopadhyay and Balasubramanian, 1993),the primary use of structural models seems to lie in the computational studies of turbulence control. An example is the study of the wall effects of the imposition of a Lorentz force vector on a sea water turbulent boundary layer (Bandyopadhyay and Balasubramanian,1994b). Because a turbulent boundary layer can be modeled by one well-defined hairpin vortex at a preferred orientation, and lying in a unit domain of turbulence production, the interaction between the applied force vector and the single vortex can be studied in a controlled manner. Similarly, the most important potential of the present structural model perhaps lies in its use in artificial neural networks to provide an accurate predictive capability of the many time-dependent quantities that define the separation process.

It is encouraging to see that a beginning has been made in the real-time prediction and modeling of an experimental flow field using neural networks (Faller et al., (1994). The integrated system of sensors, actuators, and controllers are not yet developed for a comprehensive flow control, but the following significant progress has been made. Faller et al. (1994) have considered the forced unsteady separated flow attributed to a pitching airfoil. Using arrays of known time-dependent surface-pressure signals, an artificial neural network was able to reproduce many of the characteristics of the flow-wing interactions. It is expected that this model could be the foundation upon which adaptive control systems could be built in the future.

Similar to the experimental flow field of Faller et al. (1994), incipient separation also involves a low-frequency process. Neither uses the Navier-Stokes equations to gain insight into the flow phenomenon. The key contribution of the present work is the demonstration that the process of intermittent separation is low-dimensional in character. The low-dimensional characteristics of the structural model indicate that the process of incipient separation may also be amenable to adaptive control employing artificial neural networks. The nesting nature of equation (6) is analogous to the architecture of a neural network. Commonly, in artificial neural networks, a sigmoidal function is used to model the dynamics. The present work shows that in the process of intermittent separation, equation (5) is a good choice as a model.

The model (equation (5)) may be considered to be a template for recognizing the train of large structures to come, which is the work of an instability wave of turbulence regeneration. The prediction of this incoming train in real time could lead to the detection and control of the instability waves. Eventually, controlling the instability waves would have a higher payoff than controlling the three-dimensional hairpin vortices formed by such an instability wave. Work is currently in progress on the development of micro-tiles that can apply an electromagnetic field in a sea water turbulent boundary layer for turbulence control (Bandyopadhyay, 1994). Because each of these tiles, in principle, can be programmed to be activated in space and time, conceivably, any instability wave, whose existence is known in space and time, can be canceled by applying an appropriate perturbation in an opposite phase. Because the train of large structures involved in the incipient separation process is the postcursor of the instability wave of turbulence regeneration, the present model could be helpful in the actual detection of such an instability wave.

8. CONCLUSIONS

A brief analysis and experiment on the structure of turbulence in the vicinity of a flat-plate turbulent boundary layer undergoing an intermittent separation in space have been carried out. This kind of separation is not a single event, but rather a time-dependent process spread over space. The process is not random in nature either. The quasi-organized nature of this process has been identified. The knowledge of the separation process was then distilled to develop a low-dimensional structural model of the unsteady separation process. The usefulness of the model may be enhanced by employing artificial neural networks into a subsequent turbulence control algorithm.

In the experiments conducted, laser-light sheet smoke-flow visualization was carried out to determine the structure of turbulence in the intermittently separating region. As separation is approached, the constituent hairpin vortices of the turbulent boundary layer tend to an upright posture, and the large structures pile up on each other because of a reduction in their convection velocity. Thereby, the fully turbulent core widens, and the intermittent region shrinks and moves outward compared to δ, confirming the suggestions of Fiedler and Head (1966).

This type of incipient separation on a flat plate turbulent boundary layer is a quasi-cyclic process. From the permanently separated downstream region, after the first near-wall liftup of the fluid that is rich in vorticity, the local point of separation propagates upstream while causing a train of quasi-periodic liftups of rolled-up layers of vorticity away from the wall. At the time when the point of separation has moved to the farthest upstream position, the instantaneous upstream interface of the separated region is virtually linear and resembles that of the large structures in a zero pressure gradient turbulent boundary layer. During the upstream propagation, the instantaneous separation interface is a distinct boundary between the main stream and the recirculating rotational region. Although submerged in a thick shear layer, this separation interface is also the upstream interface of the *last large structure of the main stream*. This vigorous upstream-moving part of the separation process is followed by an eventless downstream propagation of the point of separation, which completes the cycle.

The key contribution of this work is the demonstration that the process of intermittent separation is not random; rather, it is quasi-organized in nature. A low-dimensional structural model of the phenomenon of separation intermittency, which describes the measurements of separation intermittency well, was developed. The model has the following features: (1) it incorporates the observations of the organized nature of the separation process as well as that of a flat-plate turbulent boundary layer; and (2) it is nonstatistical in nature and requires only a handful of numbers of large structures (<10) to describe the phenomenon of intermittent separation. It is believed that the feature of low dimensionality makes this technologically important flow field tractable and therefore amenable to turbulence control. The model equation may be useful to artificial neural networks for predicting the turbulent boundary layer quantities that describe the separation process in real time.

The most important result of the proposed structural model is that there is a sequence of large structures involved in the separation process and that this sequence has a regular attractor. Although much remains to be investigated, the result is significant. The work shows how the features of hydrodynamics, in general, and the intermittent separation process, in particular, can be treated within the framework of nonlinear dynamics/chaos theory.

9. BIBLIOGRAPHY

Andreopoulos, J., and J. Agui (1994), "Wall-Vorticity Flux Dynamics in a Two-Dimensional Turbulent Boundary Layer," *Journal of Fluid Mechanics* (in publication).

Bandyopadhyay, P. R. (1977), "Combined Flow Visualization and Hot-Wire Anemometry in Turbulent Boundary Layers," in *Structures and Mechanism of Turbulence 1, Lecture Notes in Physics*, H. Fiedler,ed., vol. 75, pp. 205-216, Springer Verlag Publishers.

Bandyopadhyay, P. (1980), "Large Structure with a Characteristic Upstream Interface in Turbulent Boundary Layers," *Physics of Fluids*, vol. 23, no. 11, pp. 2326-2327.

Bandyopadhyay, P. R. (1983), "Turbulence Spot Like Features of a Boundary Layer," *Annals of the New York Academy of the Sciences*, vol. pp. 393-395.

Bandyopadhyay, P. R. (1986), "Aspects of the Equilibrium Puff in Transitional Pipe Flow," *Journal of Fluid Mechanics*, vol. 163, pp. 439-458.

Bandyopadhyay, P. R. (1989a), "Effect of Abrupt Pressure Gradients on the Structure of Turbulent Boundary Layers," in *Proceedings of the Tenth Australasian Fluid Mechanics Conference*, A. E. Perry ed., vol. 1, pp. 1.1-1.4, University of Melbourne, Australia.

Bandyopadhyay, P. R. (1989b), "Viscous Drag Reduction of a Nose Body," *American Institute of Aeronautics and Astronautics Journal*, vol. 27, no. 3, pp. 274-282.

Bandyopadhyay, P. R. (1991), "Instabilities and Large Structures in Reattaching Boundary Layers," *American Institute of Aeronautics and Astronautics Journal*, vol. 29, no. 7, pp. 1149-1155.

Bandyopadhyay, P. R. (1994), "Microfabricated Silicon Tiles for Electromagnetic Turbulence Control," U. S. Patent Application, Navy Case Number 76541.

Bandyopadhyay, P. R., and R. Balasubramanian. (1993), "A Vortex Model for Calculating Wall-Pressure Fluctuations in Turbulent Boundary Layers," in *Flow Noise Modeling, Measurement and Control 1993*, T. M. Farabee, W. L. Keith, and R. M. Lueptow, eds., NCA-vol. 15, FED-vol. 168, pp. 13-24.

Bandyopadhyay, P. R., and R. Balasubramanian (1994a), "Vortex Reynolds Number in Turbulent Boundary Layers," *Journal of Theoretical and Computational Fluid Dynamics*, vol. 7, no. 2 (in publication).

Bandyopadhyay, P. R., and R. Balasubramanian (1994b), "Structural Modeling of the Wall-Effects of Lorentz Force in Turbulent Wall-Bounded Flows," NUWC-NPT Technical Report 10,314, Naval Undersea Warfare Center Division, Newport, RI.

Bandyopadhyay, P. R., and R. D. Watson (1988), "Structure of Rough-Wall Turbulent Boundary Layers," *Physics of Fluids,* vol. 31. pp. 1877-1883.

Batchelor, G. K., (1967), *An Introduction to Fluid Mechanics,* Cambridge University Press.

Batchelor, G. K, and I. Proudman (1954), "The Effect of Rapid Distortion on a Fluid in Turbulent Motion," *Quarterly Journal of Mechanics and Applied Mathematics,* vol. 7, pp. 83-103.

Black, T. J. (1968), "An Analytical Study of the Measured Wall Pressure Field Under Supersonic Turbulent Boundary Layers," NASA Contractor's Report 888, National Aeronautics and Space Administration.

Corrsin, S. (1957), "Some Current Problems in Turbulent Shear Flows," in *Naval Hydrodynamics*, Publication 515.

Driver, D. M., H. L. Seegmiller, and J. G. Marvin (1987), "Time-Dependent Behavior of a Reattaching Shear Layer," *American Institute of Aeronautics and Astronautics Journal,* vol. 25, pp. 914-919.

Eaton, J. K., and J. P. Johnston (1981), "A Review of Research on Subsonic Turbulent Reattachment," *American Institute of Aeronautics and Astronautics Journal,* vol. 19, pp. 1093-1100.

Faller, W. E., S. J. Schreck, and H. E. Helin (1994), "Real-Time Prediction and Control of Three-Dimensional Unsteady Separated Flow Fields Using Neural Networks," *Paper Number AIAA 94-0532,* 32nd Aerospace Sciences Meeting, 10-13 January 1994, Reno, NV.

Fiedler, H. (1988), "Coherent Structures in Turbulent Flows," *Progress in Aerospace Sciences,* vol. 25, pp. 231-269.

Fiedler, H., and M. R. Head (1966), "Intermittency Measurements in a Turbulent Boundary Layer," *Journal of Fluid Mechanics,* vol. 25, pt. 4, pp. 719-735.

Gad-el-Hak, M., and P. R. Bandyopadhyay (1994), "Reynolds Number Effects in Wall-Bounded Turbulent Flows," *Applied Mechanics Reviews,* vol. 47, no. 8, pp. 307-365.

Gad-el-Hak, M., and D. M. Bushnell (1991), "Separation Control: Review," *Journal of Fluids Engineering, Transactions of the American Society of Mechanical Engineers*, vol. 113, pp. 5-30.

Galbraith, R. A. Mc., and M. R. Head (1975), "Eddy Viscosity and Mixing Length from Measured Boundary Layer Development," *The Aeronautical Quarterly*, vol. 26, pp. 133-154.

Glowacki, W. J., and S. W. Chi (1972), "Effect of Pressure Gradient on Mixing Length for Equilibrium Turbulent Boundary Layers," *American Institute of Aeronautics and Astronautics Conference Paper 72-213.*

Head, M. R. (1968), "Entrainment Approach," in *Short Course on Turbulent Boundary Layers,* Lecture Series 5, part 3, 4-15 March 1968, Von Kármán Institute for Fluid Dynamics, Rhode-Saint-Genese, Belgium.

Head, M. R., and P. Bandyopadhyay (1978), "Combined Flow Visualization and Hot-Wire Measurements in Turbulent Boundary Layers," in *Proceedings of the Workshop on Coherent Structure of Turbulent Boundary Layers*, C. R. Smith and D. E. Abbott, eds. , Lehigh University, pp. 98-129.

Head, M. R., and P. Bandyopadhyay (1981), "New Aspects of Turbulent Boundary-Layer Structure," *Journal of Fluid Mechanics,* vol. 107, pp. 297-338.

Lighthill, M. J. (1963), "Introduction (to) Boundary Layer Theory," in *Laminar Boundary Layers,* L. Rosenhead, ed., Dover Publishers, pp. 46-113.

Michalke, A. (1965), "Spatially Growing Disturbances in an Inviscid Shear Layer," *Journal of Fluid Mechanics,* vol. 23, no. 3, pp. 521-544.

Patel, V. C., and M. R. Head (1970), "A Simplified Version of Bradshaw's Method for Calculating Two-Dimensional Turbulent Boundary Layers," *The Aeronautical Quarterly,* vol. 21, pp. 243-262.

Perry, A. E., and M. S. Chong (1982), "On the Mechanism of Wall Turbulence," *Journal of Fluid Mechanics,* vol. 119, pp. 173-217.

Perry, A. E., T. T. Lim, and E. W. Teh (1981), "A Visual Study of Turbulent Spots," *Journal of Fluid Mechanics,* vol. 104, pp. 387-405.

Perry, A. E. and, W. H. Schofield (1973), "Mean Velocity and Shear Stress Distributions in Turbulent Boundary Layers," *Physics of Fluids,* vol. 16, no. 12, pp. 2068-2074.

Perry, A. E., J. D. Li, and I. Marusic (1991), "Towards a Closure Scheme for Turbulent Boundary Layers Using the Attached Eddy Hypothesis," *Proceedings of the Royal Society, Series A*, vol. 336, pp. 67-79.

Sandborn, V. A., and S. J. Kline (1961), "Flow Models in Boundary Layer Stall Inception," *Journal of Basic Engineering, Transactions of the American Society of Mechanical Engineers,* vol. 83, pp. 317-327.

Simpson, R. L. (1985), "Two-Dimensional Separated Turbulent Flow," A. D. Young, ed., *AGARD-AG-287* V1, Advisory Group for Aerospace Research and Development, Neuilly Sur Sein, France, pp. 1-99.

Simpson, R. L., J. H. Strickland, and P. W. Barr (1977), "Features of a Separating Turbulent Boundary Layer in the Vicinity of Separation," *Journal of Fluid Mechanics,* vol. 79, pt. 3., pp. 553-594.

Thompson, B. G. J. (1965), "A New Two-Parameter Family of Mean Velocity Profiles for Incompressible Boundary Layers on Smooth Walls," *ARC R & M 3463,* Aeronautical Research Council, United Kingdom.

Townsend, A. A. (1970), "Entrainment and the Structure of Turbulent Flow," *Journal of Fluid Mechanics,* vol. 41, pp. 31-46.

Tritton, D. J. (1988), *Physical Fluid Dynamics,* Oxford University Press.

Van Maanen, H. R. E. (1980), "Experimental Study of Coherent Structures in the Turbulent Boundary Layer of Pipe Flow Using Laser-Doppler Anemometry," in *Conference Proceedings of the Advisory Group for Aerospace Research and Development, AGARD CP 271: Turbulent Boundary Layers - Experiments, Theory and Modelling,* pp. 3.1-3.20.

Weisbrot, I. , and I. Wygnanski (1988), "On Coherent Structures in a Highly Excited Mixing Layer," *Journal of Fluid Mechanics,* vol. 195, pp. 137-159.

INITIAL DISTRIBUTION LIST

Addressee	No. of Copies
Chief of Naval Research (ONR-333 (S. Lekoudis, P. Purtell, J. Fein), ONR-334 (K. Ng))	4
Naval Research Laboratory	1
Naval Postgraduate School	1
Naval Surface Warfare Center, Carderock Division (T. Huang)	1
Naval Surface Warfare Center, Dahlgren Division	1
Defense Technical Information Center	12
Center for Naval Analyses	1
Applied Research Laboratory, Penn State U	1
NASA Lewis Research Center (K. B. M. Q. Zaman)	1
City University of New York (Professors Y. Andreopoulos and R. Raj)	2
Iowa Institute of Hydraulic Research (Professor V. C. Patel)	1
Massachusetts Institute of Technology (Professor K. S. Breuer)	1
University of Notre Dame (Professor M. Gad-el-Hak)	1
Virginia Polytechnic Institute and State University (Professor D. P. Telionis)	1
Worcester Polytechnic Institute (Professor D. P. Olinger)	1
Yale University (Professor K. R. Sreenivasan)	1